The Cryosphere Discuss., doi:10.5194/tc-2016-3, 2016
Manuscript under review for journal The Cryosphere
Published: 21 January 2016

Grounding and Calving Cycle of Mertz Ice Tongue Revealed by Shallow Mertz Bank

Xianwei Wang[1,2], David M. Holland[2,3], Xiao Cheng[1,5] and Peng Gong[4,5]

1. State Key Laboratory of Remote Sensing Science, and College of Global Change and Earth System Science, Beijing Normal University. Beijing 100875, China.
2. Center for Global Sea Level Change, New York University Abu Dhabi. Abu Dhabi, United Arab Emirates.
3. Courant Institute of Mathematical Sciences, New York University. New York 10012, United States of America.
4. Ministry of Education Key Laboratory for Earth System Modeling, and Center for Earth System Science, Tsinghua University, Beijing, China 100084.
5. Joint Centre for Global Change Studies, Beijing, China.

Correspondence to: *wangxianwei0304@163.com*

The Cryosphere Discuss., doi:10.5194/tc-2016-3, 2016
Manuscript under review for journal The Cryosphere
Published: 21 January 2016

Abstract

A recent study, using remote sensing, provided some evidence that a seafloor shoal influenced the 2010 calving event of the Mertz Ice Tongue (MIT), by partially grounding the MIT several years earlier. In this paper, we propose a method to calculate firn air content (FAC) around Mertz from seafloor-touching icebergs. Our calculations indicate the FAC around Mertz region as 4.87±1.31 m. We design an indirect method of using freeboard and sea level data extracted from ICESat/GLAS, FAC, and highly accurate seafloor topography to detect grounding sections of the MIT between 2002 and 2008 and analyze the process of grounding before the calving. By synthesizing remote sensing data, we point out that the grounding position was just localized northeast of the Mertz ice front close to the Mertz Bank. The grounding outlines of the tongue caused by the Mertz Bank are extracted as well, however the length is only limited in several kilometers since late 2002. From 2002 to 2008, the grounding area increased and the grounding became more pronounced. Additionally, the ice tongue could not climb over the Mertz Bank in following the upstream ice flow direction and that is why MIT rotated clockwise after late 2002. Furthermore, we demonstrate that the area-increasing trend of the MIT changed little after calving (~36 km^2/a), thus allowing us to use remote sensing to estimate the elapsed time until the MIT can reground on the shoal. This time period is approximately 70 years. The calving of MIT can be repeatable because of the shallow Mertz Bank and the calving cycle of the MIT explains the cycle of sea-surface condition change around Mertz.

Keywords: Mertz Ice Tongue, Firn air content, iceberg grounding, Mertz Bank, iceberg scouring, calving cycle.

The Cryosphere Discuss., doi:10.5194/tc-2016-3, 2016
Manuscript under review for journal The Cryosphere
Published: 21 January 2016

1. Introduction

Surface-warming induced calving or disintegration of floating ice has occurred in Antarctica, such as the Larsen B ice shelf (Scambos et al., 2000, 2003; Domack et al., 2005; Shepherd et al., 2003). While surface or sub-surface melting has largely been recognized to contribute to floating ice loss in Antarctica (Depoorter et al., 2013), calving caused by interaction with the seafloor has not been widely considered. The Mertz Ice Tongue (MIT) was reported to have calved in 2010, subsequent to being rammed by a large iceberg, B-9B (Legresy et al. 2010). After the calving, the areal coverage of the Mertz polynya, and sea-ice production and dense, shelf-water formation in the region changed (Kusahara et al. 2011; Tamura et al. 2012). However, the iceberg collision may have only been an apparent cause of the calving as other factors had not been fully considered such as seafloor interactions (Massom et al., 2015; Wang. 2014). By comparing inversed ice thickness to surrounding bathymetry, and combining remote sensing, Massom et al., (2015) considered that the seabed contact may have held the glacier tongue in place to delay calving by ~8 years. The interaction of the MIT and seafloor, the exact grounding location of the MIT before calving and how severe the grounding was are still not well-known.

The MIT (66 °S-68 °S, 144 °E-150 °E, Fig. 1) is located in King George V Land, East Antarctica, with an ice tongue extending over 140 km from its grounding line to the tongue front and approximately 30 km wide at the front (Legresy et al., 2004). The increasing availability over the last decade of remote sensing, hydrographic surveying, and bathymetric data allow the causes of ice tongue instability to gradually come into focus. From satellite altimetry, a modest elevation change rate of 0.03 m/a (Pritchard et al., 2012) and a freeboard change rate of -0.06 m/a (Wang et al., 2014) were found, which implied that the combined effects of surface accumulation and basal melt were not dramatic for this ice tongue. For the MIT, investigations of tidal effects, surface velocity, rift propagation, and ice front propagation (Berthier et al., 2003; Frezzotti et al., 1998; Legresy et al., 2004; Lescarmontier et al., 2012; Massom et al., 2010, 2015) have been conducted with an objective of detecting underlying factors affecting stability. Grounding as a potential factor can affect the stability of an ice tongue, as recently pointed out by Massom et al. (2015). However, without highly accurate bathymetric data, it is impossible to carry out such study. Fortunately, In 2010, a new and high resolution bathymetry model with a resolution of 100 m was released for the Terra Adelie and George V continental margin (Beaman et al., 2011), and incidentally later used to generate the Bedmap-2 (Fretwell et al., 2013). Such accurate data provides an opportunity for better exploring seafloor shoals and their impact on the instability of MIT. In this study, we focus on the grounding event of the MIT from 2002 to 2008. A method for grounding event detection will be proposed and the grounding of the MIT before calving will be investigated.

2. Data

The primary data used in this study are Geoscience Laser Altimeter System (GLAS) data onboard the Ice, Cloud and land Elevation Satellite (ICESat) and the seafloor bathymetry data mentioned above. In this section, ICESat/GLAS and bathymetry data, as well as some preprocessing are introduced.

2.1 ICESat/GLAS

The Ice, Cloud, and Land Elevation Satellite (ICESat) is the first spacebone laser altimetry satellite orbiting the Earth, lunched by National Aeronautics and Space Administration (NASA) in 2003 (Zwally et al. 2002) with Geoscience Laser Altimetry System (GLAS) as the primary payload onboard. ICESat/GLAS was operated in an orbit of ~600 km and had a geographical coverage from 86 °S to 86 °N. ICESat/GLAS usually observed in nadir viewing

The Cryosphere Discuss., doi:10.5194/tc-2016-3, 2016
Manuscript under review for journal The Cryosphere
Published: 21 January 2016

geometry and employed laser pulses of both 532 nm and 1064 nm to measure the distance from the sensor to the ground (Zwally et al. 2002). On the ground, ICESat/GLAS's footprint covered an area of approximately 70 m in diameter, with two each adjacent footprints spaced by ~170 m. The horizontal location accuracy of the footprint is about 6 m (Abshire et al. 2005). The accuracy and precision of ICESat/GLAS altimetry data are 14 cm and 2 cm respectively (Shuman et al. 2006). ICESat/GLAS usually observed two or three campaigns a year from 2003 to the end of 2009, with each campaign lasting for about one month. With billions of laser footprints received by the telescope, 15 types of data were produced for various scientific applications, named as GLA01, GLA02, … GLA15. In this study, GLA12 data (elevation data for polar ice sheet) covering the Mertz from release 33 during the interval of 2003 to 2009 is used, the spatial distribution of which is shown in Fig. 2.

2.2 Seafloor Topography

Detailed bathymetry maps are fundamental spatial data for marine science studies (Beaman et al., 2003, 2011) and crucially needed in the data-sparse Antarctic coastal region (Massom et al. 2015). Regionally, around Mertz, a large archive of ship track single-beam and multi-beam bathymetry data from 2000 to 2008 were used to generate a high resolution Digital Elevation Model (DEM), the spatial coverage of which can be found in Fig. 2 of Beaman et al. (2011) and bathymetry data coverage over the Mertz region can be found from S-Fig. 1. The DEM product was reported as having a vertical accuracy of about 11.5 m (500 m depth) and horizontal accuracy of about 70 m (500 m depth) in the poorest situation (Beaman et al. 2011). Around Antarctica, seafloor topography data from Bedmap-2 was produced by Fretwell et al. (2013) which adopted the DEM from Beaman et al. (2011). In this study, Bedmap-2 seafloor topography data covering Mertz is employed to detect the contact between seafloor and the MIT.

The Cryosphere Discuss., doi:10.5194/tc-2016-3, 2016
Manuscript under review for journal The Cryosphere
Published: 21 January 2016

Because of inconsistent elevation systems for ICESat/GLAS and seafloor topography data, the Earth Gravitational Model 2008 (EGM08) geoid with respect to World Geodetic System 1984 (WGS-84) ellipsoid is taken as reference. Since seafloor topography from Bedmap-2 is referenced to g104c geoid, elevation transformation is required and can be implemented through Eq. (1).

$$E_{sf} = E_{seafloor} + gl04c_{to\_wgs84} - EGM2008 \quad (1)$$

where 'E_{sf}' and '$E_{seafloor}$' is the seafloor topography under EGM08 and g104c respectively, '$gl04c_{to\_wgs84}$' is the value needed to convert height relative to gl04c geoid to that under WGS-84, and '*EGM2008*' is the geoid undulation with respect to WGS-84.

3. Methods

3.1 Grounding Detection Method

ICESat/GLAS data has been widely used to determine ice freeboard, or ice thickness, since its launch in 2003 (Kwok et al., 2007; Wang et al., 2011, 2014; Yi et al., 2011; Zwally et al., 2002, 2008). To study ice freeboard, draft, and grounding of the MIT in different years, ICESat/GLAS GLA12 data from release 33 from 2003 to 2009 are used, the spatial coverage of which can be seen in Fig. 2. The methods we designed for grounding detection of the MIT are now introduced briefly. First, assuming a floating ice tongue, based on freeboard data extracted in different observation dates, the ice draft of the MIT is inversed. Next, ice bottom elevation is calculated based on the inversed ice draft and the lowest sea surface height. Finally, the ice bottom is compared with seafloor topography and ice grounding is detected. The underlying logic for grounding detection is that if the inversed ice bottom is lower than seafloor, we can deny the former assumption and draw a conclusion that the ice tongue is grounded rather than floating.

The Cryosphere Discuss., doi:10.5194/tc-2016-3, 2016
Manuscript under review for journal The Cryosphere
Published: 21 January 2016

The Cryosphere Discussions

The method to extract freeboard using ICESat/GLAS from multi-campaigns over the MIT was described in Wang et al. (2014). Here, we will not revisit it in detail but introduce it schematically. According to Wang et al. (2014), four steps were included in freeboard extraction. The first step was on data preprocessing, saturation correction, data quality control, and tidal correction removal to get elevation data on the instantaneous sea surface condition. The second step was to derive sea-level height according to each track and calculate freeboard for each campaign. The third step was to relocate footprints with ice velocity. The forth step was to interpolate the freeboard map with a kriging method. With this method, freeboard map of the MIT are produced on November 14, 2002, March 8, 2004, December 27, 2006 and January 31, 2008 respectively because of known ice tongue outlines from Landsat images.

Ice draft is calculated with Eq. (2) assuming hydrostatic equilibrium and the lowest sea surface height is extracted as well from ICESat/GLAS data from all campaigns covering this region, which was -3.35 m under EGM 08 (WGS-84). In a background of changing tidal sea-surface heights, the minimum sea surface height can allow ice with a given draft to most-strongly ground to the seafloor. Then, ice bottom elevation is calculated. To compare the ice bottom with the seafloor, an elevation difference of both is calculated. In this way, a negative value indicates that ice bottom is lower than seafloor, which corresponds to a grounding phenomenon.

$$\rho_w D = \rho_i (H_f + D - FAC) \quad (2)$$

where 'D' is ice draft, i.e. vertical distance from sea surface to bottom of ice; 'H_f' is freeboard, i.e. vertical distance from sea surface to top of snow; 'ρ_w' and 'ρ_i' are densities of ocean water and ice, respectively. In this study, ice and sea water density are taken as 915 kg/m^3 and 1024 kg/m^3, respectively (Wang et al., 2014); 'FAC' is the firn air content, the decrease in thickness (in meters) that occurs when the firn column is compressed to the density of glacier ice, the same

The Cryosphere Discuss., doi:10.5194/tc-2016-3, 2016
Manuscript under review for journal The Cryosphere
Published: 21 January 2016

as what was defined in Holland et al., (2011) and Ligtenberg et al. (2014). The calculation of firn air content around Mertz will be introduced in Section 3.2. In this paper, we define the elevation of at the underside (bottom) of the tongue as 'E_{ice_bottom}' and it can be calculated by Eq. (3). Similarly, the elevation difference of ice tongue bottom and seafloor is defined as 'E_{dif}', which can be calculated by Eq. (4).

$$E_{ice\_bottom} = E_{sea\_level} - D \quad (3)$$

where 'E_{ice_bottom}' corresponds to elevation of the ice bottom. 'E_{sea_level}' is the lowest sea surface height.

$$E_{dif} = E_{ice\_bottom} - E_{sf} \quad (4)$$

where 'E_{dif}' is elevation difference by subtracting the seafloor elevation from the ice bottom.

3.2. Firn Air Content Estimation Method

The Antarctic ice sheet is covered by a dry, thick firn layer, which represents an intermediate stage between fresh snow and glacial ice, having a density between 350 km/m^3 and 900 km/m^3 (Van den Broke, 2008). The density of firn layer increases from the surface to the bottom, which usually follows an exponential distribution of depth (Patersen, 1994). Using a combination of regional climate model output and steady-state firn compaction model, the density and depth of the Antarctic firn layer has been modeled (e.g., Van den Broke, 2008). Time-dependent Firn Air Content (FAC) was also modeled by considering the physical process of firn layer (e.g., Ligtenberg et al. 2014). For the MIT, there are some in-situ measurements of snow thickness available from Massom et al. (2010) who used a snow layer depth of 1 m to derive the thickness of surrounding multi-year fast sea ice. However on the surface of the MIT, no in-situ measurements of density and depth of firn layer are available.

The Cryosphere Discuss., doi:10.5194/tc-2016-3, 2016
Manuscript under review for journal The Cryosphere
Published: 21 January 2016

To invert glacial ice thickness from freeboard observation under hydrostatic assumption, one can use a two-layer density model, which consists of an upper firn layer and a lower glacial layer (Luckman et al., 2010). In the upper layer, firn density varies with depth. However, in the lower glacial layer, the density is considered a constant. One can also use FAC to correct the inversed ice thickness assuming hydrostatic equilibrium (Rignot and Jacobs, 2002). In this study, we use FAC extracted from adjacent seafloor-touching icebergs to investigate the grounding of the MIT rather than FAC from modeling.

From Smith (2011), icebergs can be divided into three categories based on topography and seasonal pack ice distributions: grounded iceberg, constrained iceberg, and free-drifting iceberg. Without occurrence of pack ice, an iceberg can be free-drifting or grounded. Free-drifting iceberg can move several tens of kilometers per day, such as iceberg A-52 (Smith et al. 2007). Grounded icebergs can be firmly or lightly anchored. Heavily grounded icebergs have firm contact with the seafloor and can be stationary for a long time, such as iceberg B-9B (Massom. 2003). However, slightly grounded icebergs may have little contact with the seafloor and can possibly move slowly under the influence of ocean tide, ocean currents or winds, but much slower than free-drifting icebergs. The relation of grounding and ice drifting velocity is not well-known. However, from slowly drifting or nearly stationary icebergs in open water, we can determine if an iceberg is grounded.

Because of the heavily grounded iceberg B-9B to the east of the MIT blocking the drifting of pack ice or icebergs from the east, icebergs located between B-9B and the MIT are most likely generated from the Mertz or Ninnis glaciers. We can calculate the FAC from these icebergs and apply it to grounding event detection of the MIT, in terms of estimating the FAC of the MIT itself. Around the MIT, locations of three icebergs (‘A’, ‘B’ and ‘C’) were identified

The Cryosphere Discuss., doi:10.5194/tc-2016-3, 2016
Manuscript under review for journal The Cryosphere
Published: 21 January 2016

using MODIS and Landsat images in austral summer, 2006 and 2008 and shown in Fig. 6. Fortunately, ICESat/GLAS observed these icebergs on February 23, 2006 (54th day of 2006) and February 18, 2008 (49th day of 2008). These allow us to analyze the behavior of the icebergs three-dimensionally. From Fig. 4a, icebergs 'A', 'B' and 'C' changed position little in about two months (from 28 to 85 day of 2006). Thus we can consider these icebergs slightly grounded. These slightly grounded icebergs may plough the seafloor and leave ridges or grooves. In Pine Island Trough, ridges on the seafloor have been already found with a range of 1 to 2 m, which was believed to be influenced by tides (Jakobsson et al. 2011; Woodworth-Lynas et al. 1991). From this viewpoint, we are confident that under the lowest sea level (lowest tide), these iceberg must be grounded, which means that the ice draft inversed from freeboard measurement assuming hydrostatic equilibrium must be greater than or equal to water depth. Based on this analysis, we can take water depth as draft to calculate the FAC and the FAC calculated with this method should be less than or equal to the absolute value.

Because only 'A' and 'C' were observed by track 1289 of the ICESat/GLAS in 2006, freeboard and water depth from bathymetry for both are used to calculate the FAC. However, the icebergs were not stationary, which indicates only some parts were grounded. In this study, only the top two largest measurements of each freeboard profile are employed to calculate the FAC with Eq. (2) with least square method under hydrostatic equilibrium. The result is listed in Table 1.

From Table 1, we can find the average FAC is about 4.87±1.31 m. Under this FAC setting, the accuracy of grounding detection with this method is about ±11 m (one standard deviation of the residuals). Two icebergs observed by the same track of the ICESat/GLAS on February 18, 2008 are used to evaluate the grounding detection using this FAC result. From

The Cryosphere Discuss., doi:10.5194/tc-2016-3, 2016
Manuscript under review for journal The Cryosphere
Published: 21 January 2016

positions observed by remote sensing in Fig. 4b, we know, iceberg 'A' drifted away from its original position. Thus it was not grounded. Iceberg 'B' kept rotating in this period without drifting away, which we can consider it grounded. The elevation difference of ice bottom and seafloor is shown in Table 1, from which we can see that a grounding iceberg 'B' and floating iceberg 'A' is clearly identified. Thus the FAC estimation works well around Mertz.

Actually, for FAC calculation, icebergs just touching the seafloor should be used, in which case, the FAC calculated assuming hydrostatic equilibrium is the same as the actual value. However, it is difficult to ascertain whether an iceberg is just touching the seafloor from remote sensing images. The near stationary or slowly rotating iceberg detected should be grounded more severely than one just touching the seafloor, which results in a calculated FAC theoretically larger than the actual value. Thus using this FAC result to detect grounding can lead to smaller grounding results. However, once an iceberg or ice tongue is detected as grounded, the result should be robust.

4. Accuracy Prediction for Grounding Detection

The accuracy of 'E_{dif}' is critical to grounding detection of the MIT. From Eq. (1) to (4), we can find different components of the error sources, such as errors from sea surface height determination, ice draft, seafloor bathymetry, and elevation transformation. Meanwhile, uncertainty of ice draft is primarily determined by that of freeboard and '*FAC*'. Furthermore, the uncertainty of freeboard is influenced by footprint relocation and freeboard changing rates. Considering all mentioned above, the error source of elevation difference 'E_{dif}' can be synthesized by Eq. (5):

$$\Delta E_{dif} = \Delta E_{sl} + a(\Delta H_f + \Delta E_{re} + \Delta E_{fb\_c} + \Delta FAC) + \Delta E_{sf} + \Delta E_{trans} \quad (5)$$

The Cryosphere Discuss., doi:10.5194/tc-2016-3, 2016
Manuscript under review for journal The Cryosphere
Published: 21 January 2016

where $a = \frac{\rho_i}{\rho_w - \rho_i}$; 'Δ' stands for error of each variable; 'ΔE_{dif}' stands for error of final elevation difference of ice bottom and seafloor; 'ΔE_{sl}', 'ΔH_f', 'ΔE_{re}', 'ΔE_{fb_c}', 'ΔFAC', 'ΔE_{sf}' and 'ΔE_{trans}' stand for errors caused by sea surface height extraction, freeboard extraction, freeboard relocation, freeboard changing rates, FAC calculation, seafloor bathymetry and elevation system transformation, respectively.

Usually, the influence of elevation system transformation on final elevation difference can be neglected. Based on the error propagation law, the uncertainty of elevation difference 'E_{dif}' can be described by Eq. (6):

$$\varepsilon E_{dif} = \sqrt{(\varepsilon E_{sl})^2 + a^2[(\varepsilon H_f)^2 + (\varepsilon E_{re})^2 + (\varepsilon E_{fb\_c})^2 + (\varepsilon FAC)^2] + (\varepsilon E_{sf})^2} \quad (6)$$

where 'ε' indicates uncertainty of each parameter.

Since sea level is extracted from ICESat/GLAS data track by track, we use ±0.15 m as uncertainty of elevation data ('εE_{sl}'). Also from Wang et al. (2014), we can see the uncertainty of freeboard extraction ('εH_f') is ±0.50 m. From Rignot et al. (2011), the error of ice velocity here ranged from 5 m/a to 17 m/a. Assuming that ice velocity varied by 17 m/a (an upper threshold), the relocation error horizontally could reach ±54 m in an average of three years' time. Wang et al. (2014) extracted the average slope of the MIT along ice flow direction as 0.00024. However, because of large crevasses on the surface, we use 50 times of this value as an average slope. In this way, we can estimate 'εE_{re}' as ±0.65 m when consider a three-year period. The annual changing rate of freeboard from 2003 to 2009 is -0.06 m/a (Wang et al. 2014). Therefore, we consider the freeboard stable in this period. However, when combining data from different time periods then 'εE_{fb_c}' is estimated as about ±0.18 m if considering three years' time difference. From Beaman et al. (2011), considering elevation uncertainty at the worst situation

The Cryosphere Discuss., doi:10.5194/tc-2016-3, 2016
Manuscript under review for journal The Cryosphere
Published: 21 January 2016

when water depth is 500 m, 'εE_{g104c}' is ±11.5 m. Using all these errors above, we calculate the final uncertainty of elevation difference as ±17 m.

From the calculations above, we can say that 'E_{dif}' less than -17 m corresponds to a very robust grounding event. However, if the 'E_{dif}' is greater than 17 m, we can confirm no grounding there. 'E_{dif}' in the interval of -17m to 17 m corresponds to slight grounding or floating. We can also determine different contributions of each separate factor to the overall accuracy. Seafloor bathymetry contributes the largest part and is the dominant factor affecting the accuracy of grounding detection.

5. Grounding Detection Results

The spatial distribution of elevation difference 'E_{dif}' and outline of the MIT from 2002 to 2008 can be found in Fig. 5. A buffer region with buffer radius of 2 km (region between black and grey line in Fig. 5) is also introduced to investigate grounding potential of the MIT, if it approached there. The elevation difference less than 34 m (twice of elevation difference uncertainty 'εE_{dif}') both inside and outside of the outline is extracted and the corresponding statistics are shown in Table 2. Since the uncertainty to determine a grounding event is about ± 17m, if some grids of the MIT have elevation difference 'E_{dif}' less than 17 m, we can conclude that this section of the tongue is grounded. The smaller the 'E_{dif}', the more robust the grounding. From the color-change patterns of Fig. 5a-d, we can see that part of the ice front grounded on shallow Mertz Bank from the end of 2002.

As illustrated from Table 2, the minimum'E_{dif}' inside of the MIT are all less than 17 m and the mean and minimum of the 'E_{dif}' in the buffer region are all less than 0 from 2002 to 2008. From this, we can conclude that the ice tongue has grounded on the shallow Mertz Bank since November 14, 2002. This result coincides with findings from Massom et al. (2015) who considered that the northwestern extremity of the MIT started to contact with the seafloor shoal in late 2002 to early 2003. Also it would be hard for the MIT to approach the buffer region (indicated with yellow to red color in Fig. 5) as the surrounding Mertz Bank gets shallower and steeper and substantive grounding would happen if it moved into these regions. Inside of the MIT, the minimum of elevation difference was just 11.9 m on November 14, 2002, which indicates little to no grounding. However on March 8, 2004, December 27, 2006, and January 31, 2008, the minimum of elevation difference reached -46.0 m, -52.3 m and -34.8m respectively, which means significant grounding occurred in some regions. Additionally, the mean of 'E_{dif}' inside of the tongue gradually decreases from 25.0 m to -0.8m, according to which we can conclude that the ice front was grounded more significantly with passing time. Additionally, since the grounding area increased from 6 km^2 to 13 km^2 (Table 2) and the mean of 'E_{dif}' decreased from 2002 to 2008, we can say that over the period from 2002 to 2008, the grounding of the northwest flank of the MIT became more widespread.

Based on the calculated elevation difference, the grounding outlines of the MIT are delineated on November 14, 2002, March 8, 2004, December 27, 2006 and January 31, 2008, respectively (Fig. 6). For the grounding part of the outline in different years, starting and ending location and perimeter are also extracted, from which we can conclude that the length of grounding outline because of the Mertz Bank is only limited to a few kilometers (Table 3).

We find that the lower right (northwest) of the MIT was always grounded. However, grounding did not occur in other regions (Fig. 5). The shallowest seafloor elevation the ice front touched was ~ -290 m in November 2002. In 2004, 2006 and 2008, the lower right (northwest) of the MIT even approached contour of –220 m. Fig. 6 also show the extension line of west flank in November, 2002, from which we can see that if the ice tongue moved along the former

The Cryosphere Discuss., doi:10.5194/tc-2016-3, 2016
Manuscript under review for journal The Cryosphere
Published: 21 January 2016

direction, the ice flow would be seriously blocked when approaching the Mertz Bank. The shallowest region of the Mertz Bank ahead has an elevation of about -140 m and the MIT would have needed to climb over 140 m to cross past it. The shallow Mertz Bank would have caused grounding during the climbing. This special feature of seafloor shoal facing the MIT can further explain why the ice velocity differed along the east and west flanks of the MIT before calving and why the ice tongue moved clockwise to the east, as pointed out by Massom et al. (2015). However, because of sparsely-distributed bathymetry data (point measurements) in Mertz region used in Massom et al. (2015), this effect could not be easily seen. Here, from our grounding detection results and surrounding high-accuracy bathymetry data, this effect is more clearly observed.

6. Discussion

6.1 Area Changing Rate and ~70-year Calving Cycle of MIT

Using Landsat TM/ETM+ images from 1989 to 2013, outlines of the MIT are extracted manually. Assuming a fixed grounding line position over this period, the area of the MIT over this period is calculated. Using these data, from 1989 to 2007, an area-increasing trend of the MIT is shown (from 5453 km^2 to 6126 km^2) in Fig. 7. However, the area of the MIT was almost constant from 2007 to 2010, before calving. The largest area of the MIT was 6113 km^2 closest to the calving event in 2010. After the calving, the area decreased to 3617 km^2 in November 2010.

The area-expanding trend for the MIT from 1989 to 2007 is also obtained using a least-squares method, giving a value of 35.3 km^2/a. However, after the calving a slight higher area-increasing trend of 36.9 km^2/a, is found (Fig. 7). On average, the area-increasing rate of the MIT was 36 km^2/a.

The Cryosphere Discuss., doi:10.5194/tc-2016-3, 2016
Manuscript under review for journal The Cryosphere
Published: 21 January 2016

The surface behavior such as ice flow direction changes and middle rift changes caused by grounding was analyzed by Massom et al. (2015). In the history of the MIT, one or two large calving events were suspected to have happened between 1912 and 1956 (Frezzotti et al., 1998) and we consider it likely to be only once because of the influence of the shallow Mertz Bank. When the ice tongue touched the bank, the bank started to affect the stability of the tongue by bending the ice tongue clockwise to the east, as can be seen from velocity changes from Massom et al. (2015). With continuous momentum and flux input from upstream, a large rift from the west flank of the tongue would ultimately have to occur and could potentially calve the tongue. A sudden length shortening of the tongue can be caused by such ice tongue calving as indeed had happened in February, 2010. We also consider that even without a sudden collision of iceberg B-9B in 2010, the ice tongue would eventually calve because of existence of the shallow Mertz Bank.

If we take 6127 km^2 as the maximum area of the MIT, assuming a constant area-changing rate of about 36.9 km^2/a after 2010, it will take about 68 years to calve again. When assuming an area changing rate of about 35.3 km^2/a as before 2010, it will take a little longer, about 71 years. Therefore, without considering accidental event such as collision with other large icebergs, the MIT is predicted to calve again in ~70 years. Because of the continuous ice flow upstream, the special location and relatively lower depth of the Mertz Bank, the calving is likely repeatable and a cycle therefore does exist.

After the MIT calved in February, 2010, Mertz polynya size, sea ice production, sea ice coverage and high-salinity shelf water formation changed. A sea ice production decrease of about 14-20% was found by Tamura et al. (2012) using satellite data and high-salinity shelf water export was reported to reduce up to 23% using a state-of-the-art ice-ocean model

(Kusahara et al. 2010). Recently, Campagne et al. (2015) pointed out a ~70-year cycle of surface ocean condition and high-salinity shelf water production around Mertz through analyzing reconstructed sea ice and ocean data over the last 250 years. They also mentioned that this cycle was closely related to presence and activity of Mertz polynya. However, the reason for this cycle was not fully understood.

From these findings addressed above and MIT calving cycle we found, our explanation is that calving cycle of the MIT leads to the ~70-year cycle of surface ocean condition and high-salinity shelf water production around Mertz. Calving decreases the length of the MIT suddenly. A short ice tongue reduces the size of Mertz Polynya formed by Antarctic katabatic winds and results in lower sea ice production and further lessens high-salinity shelf water production. Therefore, the cycle of ocean conditions around Mertz found by Campagne et al. (2015) is dominated by the calving of the MIT. Additionally, the cycles of MIT calving and surface ocean condition around Mertz coincides with each other well, ~70 years, which make the explanation much exact.

6.2 Iceberg Scouring Detection

Icebergs play an important role in sediment transport and distribution. Also grounded iceberg can scour the seafloor and disturb the benthic communities on parts of the Antarctic continental shelf. Iceberg scouring across the George V shelf was detected by Post et al. (2011). A recent marine science voyage to the Mertz glacier region was conducted onboard the Australian Antarctic research vessel Aurora Australis in 2011 and one objective of this voyage was to investigate benthic community composition in iceberg scours (Smith and Riddle. 2011). A camera station was set around the Mertz Bank in an attempt to detect iceberg scours caused by the MIT. However, the photos collected from this station indicated no scours. The grounding of

The Cryosphere Discuss., doi:10.5194/tc-2016-3, 2016
Manuscript under review for journal The Cryosphere
Published: 21 January 2016

the Mertz ice front on the Mertz Bank can leave scours but the camera station was far from grounding regions of the ice tongue by several kilometers. Since the tongue did not move across that place, it is unlikely to find recent scours. We suggest possible new scours detection along the margin of the grounding ice tongue as indicated with thick lines in Fig. 6.

7. Conclusion

In this study, a method of FAC calculation from seafloor-touching icebergs around Mertz region was presented. The FAC around the Mertz is about 4.87±1.31 m. This FAC is used to calculate ice draft based on sea level and freeboard extracted from ICESat/GLAS and appears to work well. A method to extract grounding sections of the MIT was described based on comparing inversed ice draft assuming hydrostatic equilibrium with seafloor bathymetry. The final grounding results explain the surface behavior of the MIT. Previous work by Massom et al. (2015) has also provided some evidence for seafloor interaction, in showing that the MIT front had an approximate 280 m draft with the nearby seafloor as shallow as 285 m, suggesting the possibility of grounding. In our work, we have provided ample detailed bathymetry and ice draft calculations. Specifically, ice bottom elevation was inversed using ICESat/GLAS data and compared with seafloor bathymetry during 2002, 2004, 2006, and 2008. From those calculations we show conclusively that MIT was indeed grounded along a specific portion of its northwest flank over a limited region. We also pointed out that even without collision by iceberg B-9B in early 2010 the ice tongue would eventually have calved because of momentum and flux input from the upstream glacier flow being increasingly opposed by a reaction force from the shoal of the Mertz Bank.

From remote sensing images we were able to quantify the rate of increase of area of the MIT before and after the 2010 calving. While the area-increasing trend of the MIT after calving

The Cryosphere Discuss., doi:10.5194/tc-2016-3, 2016
Manuscript under review for journal The Cryosphere
Published: 21 January 2016

is slightly larger than before, we used the averaged rate to estimate a timescale required for the MIT to re-advance to the area of the shoaling bathymetry from its retreated, calved position. Our estimate is ~70-years, which is remarkably consistent with Campagne et al. (2015) who found a similar period of sea surface changes using seafloor sediment data. A novel point we bring out in our study is that it is the shoaling of the seafloor combined with the rate of advance of the MIT that leads to the 70-year repeat cycle. Also the calving cycle of the MIT explains cycle of sea surface condition change well, which indicates the calving of the MIT is dominant factor for sea surface condition change. Understanding the mechanism underlying the periodicity of MIT calving is important as the presence or absence of the MIT has a profound impact on sea ice and hence of bottom water formation in the local region.

Acknowledgements

This research was supported by Fundamental Research Fund for the Central University, the Center for Global Sea Level Change (CSLC) of NYU Abu Dhabi (Grant no: G1204), the Open Fund of State Key Laboratory of Remote Sensing Science (Grant no: OFSLRSS201414), and the China Postdoctoral Science Foundation (Grant no: 2012M520185, 2013T60077). We are grateful to the Chinese Arctic and Antarctic Administration, the European Space Agency for free data supply under project C1F.18243, the National Snow and Ice Data Center for the availability of the ICESat/GLAS data (http://nsidc.org/data/order/icesat-glas-subsetter) and MODIS image archive over the Mertz glacier (http://nsidc.org/cgi-bin/modis_iceshelf_archive.pl), British Antarctica Survey for providing Bedmap-2 seafloor topography data (https://secure.antarctica.ac.uk/data/bedmap2/), the National Geospatial-Intelligence Agency for publicly released EGM2008 GIS data (http://earth-info.nga.mil/GandG/wgs84/gravitymod/egm2008/egm08_gis.html), and the USGS for Landsat data (http://glovis.usgs.gov/). Also fruitful discussions with M. Depoorter, P. Morin, T. Scambos and R. Warner are acknowledged.

References

1. Beaman, R. J., & Harris, P. T. (2003). Seafloor morphology and acoustic facies of the George V Land shelf. *Deep Sea Research Part II: Topical Studies in Oceanography*, 50(8), 1343-1355.
2. Beaman, R. J., O'Brien, P. E., Post, A. L., & De Santis, L. (2011). A new high-resolution bathymetry model for the Terre Adélie and George V continental margin, East Antarctica. *Antarctic Science*, 23(01), 95-103.
3. Berthier, E., Raup, B., & Scambos, T. (2003). New velocity map and mass-balance estimate of Mertz Glacier, East Antarctica, derived from Landsat sequential imagery. *Journal of Glaciology*, 49(167), 503-511.
4. Ballantyne, J., 2002. A multidecadal study of the number of Antarctic icebergs using scatterometer data. Brigham Young University online report: 〈http://www.scp.byu.edu/data/iceberg/IcebergReport.pdf〉.
5. Campagne, P., Crosta, X., Houssais, M. N., Swingedouw, D., Schmidt, S., Martin, A., ... & Massé, G. (2015). Glacial ice and atmospheric forcing on the Mertz Glacier Polynya over the past 250 years. *Nature Communications*, 6.
6. Depoorter, M. A., Bamber, J. L., Griggs, J. A., Lenaerts, J. T. M., Ligtenberg, S. R. M., van den Broeke, M. R., & Moholdt, G. (2013). Calving fluxes and basal melt rates of Antarctic ice shelves. *Nature*, 502(7469), 89-92.

7. Domack, E., Duran, D., Leventer, A., Ishman, S., Doane, S., McCallum, S., ... & Prentice, M. (2005). Stability of the Larsen B ice shelf on the Antarctic Peninsula during the Holocene epoch. *Nature*, 436(7051), 681-685.
8. Fretwell, P., Pritchard, H. D., Vaughan, D. G., Bamber, J. L., Barrand, N. E., Bell, R., ... & Fujita, S. (2013). Bedmap2: improved ice bed, surface and thickness datasets for Antarctica. *Cryosphere*, 7(1).
9. Frezzotti, M., Cimbelli, A., & Ferrigno, J. G. (1998). Ice-front change and iceberg behaviour along Oates and George V Coasts, Antarctica, 1912-96. *Annals of Glaciology*, 27, 643-650.
10. Fricker, H. A., Young, N. W., Allison, I., & Coleman, R. (2002). Iceberg calving from the Amery ice shelf, East Antarctica. *Annals of Glaciology*, 34(1), 241-246.
11. Griggs, J. A., & Bamber, J. L. (2011). Antarctic ice-shelf thickness from satellite radar altimetry. *Journal of Glaciology*, 57(203), 485-498.
12. Jakobsson, M., Anderson, J. B., Nitsche, F. O., Dowdeswell, J. A., Gyllencreutz, R., Kirchner, N., ... & Majewski, W. (2011). Geological record of ice shelf break-up and grounding line retreat, Pine Island Bay, West Antarctica. *Geology*, 39(7), 691-694.
13. Jenkins, A., Dutrieux, P., Jacobs, S. S., McPhail, S. D., Perrett, J. R., Webb, A. T., & White, D. (2010). Observations beneath Pine Island Glacier in West Antarctica and implications for its retreat. *Nature Geoscience*, 3(7), 468-472.
14. Joughin, I., & Alley, R. B. (2011). Stability of the West Antarctic ice sheet in a warming world. *Nature Geoscience*, 4(8), 506-513.
15. Kusahara, K., Hasumi, H. & Williams, G. D. (2011), Impact of the Mertz Glacier Tongue calving on dense water formation and export. *Nature communications*, 2, 159.

The Cryosphere Discuss., doi:10.5194/tc-2016-3, 2016
Manuscript under review for journal The Cryosphere
Published: 21 January 2016

16. Kern, S., & Spreen. G. (2015), Uncertainties in Antarctic sea-ice thickness retrieval from ICESat. *Annals of Glaciology*, 56(69), 107.

17. Kwok, R. Cunningham, G. F., Zwally, H. J., & Yi, D. (2007). Ice, Cloud, and land Elevation Satellite (ICESat) over Arctic sea ice: retrieval of freeboard. *Journal of Geophysical Research*, 112, C12013, doi:10.1029/2006JC003978.

18. Legresy, B., Wendt, A., Tabacco, I. E., Remy, F., & Dietrich, R. (2004). Influence of tides and tidal current on Mertz Glacier, Antarctica. *Journal of Glaciology*, 50(170), 427-435.

19. Legresy, B., N. Young, L. Lescarmontier, R. Coleman, R.Massom, B. Giles, A. Fraser, R. Warener, B. Galton-Fenzi, L. Testut, M. Houssais and G. Masse (2010), CRAC!!! in the Mertz Glacier, Antarctica. http://www.antarctica.gov.au/__data/assets/pdf_file/0004/22549/ml_402353967939815_mertz_final_100226.pdf

20. Lescarmontier, L., Legrésy, B., Coleman, R., Perosanz, F., Mayet, C., & Testut, L. (2012). Vibrations of Mertz glacier ice tongue, East Antarctica. *Journal of Glaciology*, 58(210), 665-676.

21. Ligtenberg, S. R. M., Heilsen, M. M., & van de Broeke, M. R. (2011). An improved semi-empirical model for the densification of Antarctic firn. *The Cryosphere*, 5(4), 809-819.

22. Ligtenberg, S., Kuipers Munneke, P., & Van Den Broeke, M. R. (2014). Present and future variations in Antarctic firn air content. *The Cryosphere*, 8(5), 1711-1723.

23. Luckman, A., Padman, L., & Jansen, D. (2010). Persistent iceberg groundings in the western Weddell Sea, Antarctica. *Remote Sensing of Environment*, 114(2), 385-391.

The Cryosphere Discuss., doi:10.5194/tc-2016-3, 2016
Manuscript under review for journal The Cryosphere
Published: 21 January 2016

24. Massom, R. A. (2003). Recent iceberg calving events in the Ninnis Glacier region, East Antarctica. *Antarctic Science*, 15(02), 303-313.

25. Massom, R. A., Giles, A. B., Fricker, H. A., Warner, R. C., Legrésy, B., Hyland, G., Young, N., & Fraser, A. D. (2010). Examining the interaction between multi-year landfast sea ice and the Mertz Glacier Tongue, East Antarctica: Another factor in ice sheet stability? *Journal of Geophysical Research*, 115, C12027, doi:10.1029/2009JC006083.

26. Massom, R. A., Giles, A. B., Warner, R. C., Fricker, H. A., Legrésy, B., Hyland, G., ... & Young, N. (2015). External influences on the Mertz Glacier Tongue (East Antarctica) in the decade leading up to its calving in 2010. *Journal of Geophysical Research: Earth Surface*, 120(3), 490-506.

27. Pavlis, N. K., Holmes S. A., Kenyon, S. C., & Factor, J. K. (2012). The development and evaluation of the Earth Gravitational Model 2008 (EGM2008), *Journal of Geophysical Research*. 117, B04406, doi:10.1029/2011JB008916.

28. Porter-Smith, R. (2003). Bathymetry of the George Vth Land shelf and slope. *Deep Sea Research Part II: Topical Studies in Oceanography*, 50(8), 1337-1341.

29. Post, A. L., Beaman, R. J., O'Brien, P. E., Eléaume, M., & Riddle, M. J. (2011). Community structure and benthic habitats across the George V Shelf, East Antarctica: trends through space and time. *Deep Sea Research Part II: Topical Studies in Oceanography*, 58(1), 105-118.

30. Pritchard, H. D., Ligtenberg, S. R. M., Fricker, H. A., Vaughan, D. G., Van den Broeke, M. R., & Padman, L. (2012). Antarctic ice-sheet loss driven by basal melting of ice shelves. *Nature*, 484(7395), 502-505.

The Cryosphere Discuss., doi:10.5194/tc-2016-3, 2016
Manuscript under review for journal The Cryosphere
Published: 21 January 2016

31. Rignot, E., Mouginot, J. & Scheuchl, B. (2011), Ice flow of the Antarctic ice sheet. *Science*, 333(6048), 1427-1430.

32. Rignot, E., & Jacobs, S. S. (2002). Rapid bottom melting widespread near Antarctic ice sheet grounding lines. *Science*, 296(5575), 2020-2023.

33. Scambos, T. Hulbe, A., C. & Fahnestock, M. A. (2003). Climate-induced ice shelf disintegration in the Antarctic Peninsula. *Antarctic Research Series*, 79, 79-92.

34. Scambos, T. Hulbe, A., C. Fahnestock, M. A. & Bohlander, J. (2000). The link between climate warming and breakup of ice shelves in the Antarctic Peninsula. *Journal of Glaciology*, 46(154), 516-530.

35. Shepherd, A., Wingham, D., Payne, T., & Skvarca, P. (2003). Larsen Ice Shelf has progressively thinned. *Science*, 302(5646), 856-859.

36. Smith, J., & Riddle, M. (2011). Benthic Community Survey, Mertz Glacier Region, East Antarctica: Post Survey Report, RSV Aurora Australis, Marine Science Voyage (2010/11 VMS), January-February 2011. Geoscience Australia.

37. Smith, K. L., Robison, B. H., Helly, J. J., Kaufmann, R. S., Ruhl, H. A., Shaw, T. J., ... & Vernet, M. (2007). Free-drifting icebergs: hot spots of chemical and biological enrichment in the Weddell Sea. *Science*, 317(5837), 478-482.

38. Smith, K. L. (2011). Free-drifting icebergs in the Southern Ocean: an overview. *Deep Sea Research Part II: Topical Studies in Oceanography*, 58(11), 1277-1284.

39. Tamura, T., Williams, G. D., Fraser, A. D. & Ohshima, K. I. (2012). Potential regime shift in decreased sea ice production after the Mertz Glacier calving, *Nature communications*, 3, 826.

40. Tchernia, P. A. U. L., & Jeannin, P. F. (1984). Circulation in Antarctic waters as revealed by iceberg tracks 1972–1983. *Polar Rec*, 22(138), 263-269.

41. Van de Berg, W. J., Van den Broeke, M. R., Reijmer, C. H., & Van Meijgaard, E. (2005). Characteristics of the Antarctic surface mass balance, 1958–2002, using a regional atmospheric climate model. *Annals of glaciology*, 41(1), 97-104.

42. Van de Berg, W. J., Van den Broeke, M. R., Reijmer, C. H., & Van Meijgaard, E. (2006). Reassessment of the Antarctic surface mass balance using calibrated output of a regional atmospheric climate model. *Journal of Geophysical Research: Atmospheres* (1984–2012), 111(D11).

43. Van den Broeke, M. (2008). Depth and density of the Antarctic firn layer. Arctic, Antarctic, and Alpine Research, 40(2), 432-438.

44. Wang, X.W., Cheng, X., Gong, P., Huang, H. B., Li Z., & Li, X. W. (2011). Earth Science Applications of ICESat/GLAS: a Review. *International Journal of Remote Sensing*, 32, 23, 8837-8864, doi: 10.1080/01431161.2010.547533

45. Wang, X.W., Cheng, X., Gong, P., Shum, C. K., Holland, D.M., & Li, X.W. (2014). Freeboard and mass extraction of the disintegrated Mertz Ice Tongue with remote sensing and altimetry data. *Remote Sensing of Environment*, 144, 1-10.

46. Wang, X.W. (2014). Mertz ice tongue evolutions from satellite observed data, Postdoctoral Research Report, College of Global Change and Earth System Science, Beijing Normal University, China. doi: 10.13140/2.1.1006.1603

47. Woodworth-Lynas, C. M. T., Josenhans, H. W., Barrie, J. V., Lewis, C. F. M., & Parrott, D. R. (1991). The physical processes of seabed disturbance during iceberg grounding and scouring. *Continental Shelf Research*, 11(8), 939-961.

48. Yi, D., Zwally, H.J., & Robbins, J. (2011). ICESat observations of seasonal and interannual variations of sea-ice freeboard and estimated thickness in the Weddell Sea, Antarctica (2003-2009). *Annals of Glaciology*, 52(57), 43-51.

49. Zwally, H. J., Schutz, B., Abdalati, W., Abshire, J., Bentley, C., Brenner, A., Buftona, J., Deziof, J., Hancocka, D., Hardinga, D., Herringg, T., Minsterh, B., Quinng, K., Palmi, S., Spinhirnea, J., & Thomasj, R. (2002). ICESat's laser measurements of polar ice, atmosphere, ocean, and land. *Journal of Geodynamics*, 34, 405-445.

50. Zwally, H. J., Yi, D., Kwok, R., & Zhao, Y. (2008). ICESat measurements of sea ice freeboard and estimates of sea ice thickness in the Weddell Sea. *Journal of Geophysical Research*, 113, C02S15, doi:10.1029/2007JC004284.

The Cryosphere Discuss., doi:10.5194/tc-2016-3, 2016
Manuscript under review for journal The Cryosphere
Published: 21 January 2016

567 **Figures**

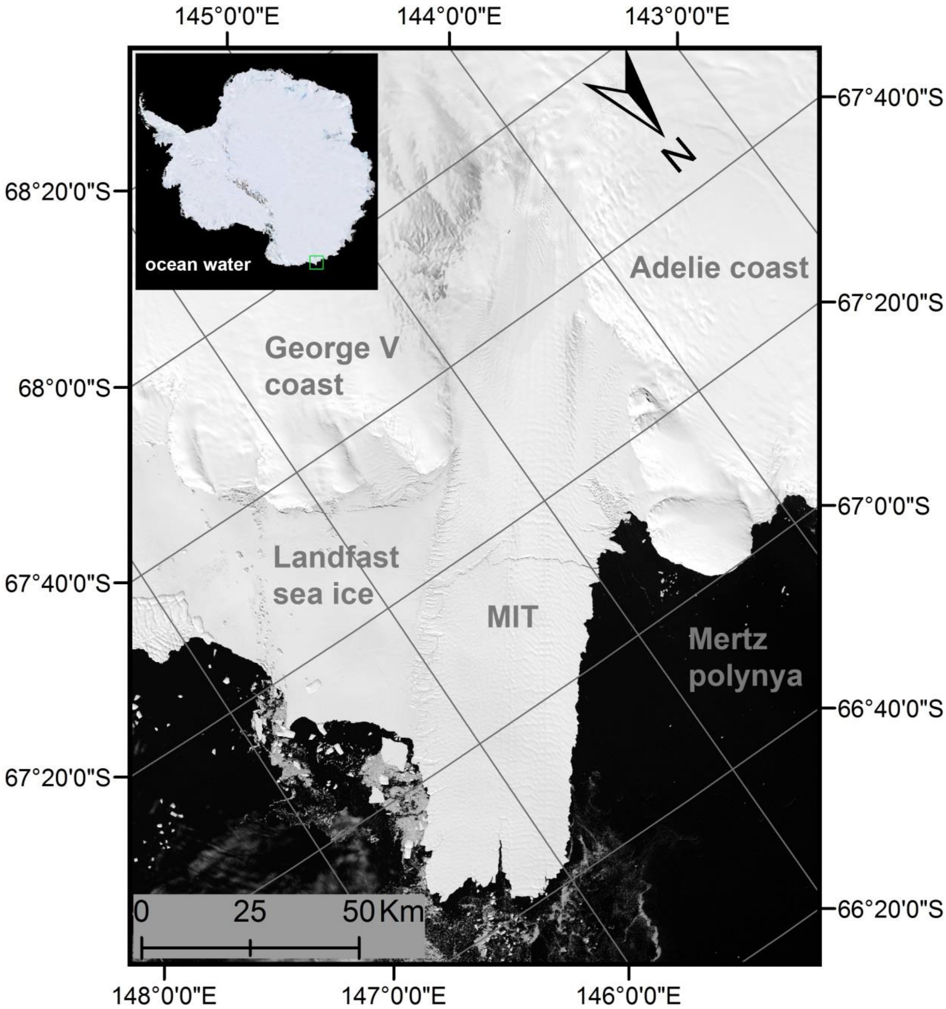

568

569 **Figure 1.** Mertz Ice Tongue (MIT), East Antarctica. Landfast sea ice is attached to the east flank
570 of the MIT and the Mertz Polynya is to the west. The background image is from band 4 Landsat
571 7, captured on February 2, 2003. The green square found in the upper left inset indicates the
572 location of the MIT in East Antarctica. A polar stereographic projection with -71 °S as standard
573 latitude is used.

The Cryosphere Discuss., doi:10.5194/tc-2016-3, 2016
Manuscript under review for journal The Cryosphere
Published: 21 January 2016

The Cryosphere Discussions

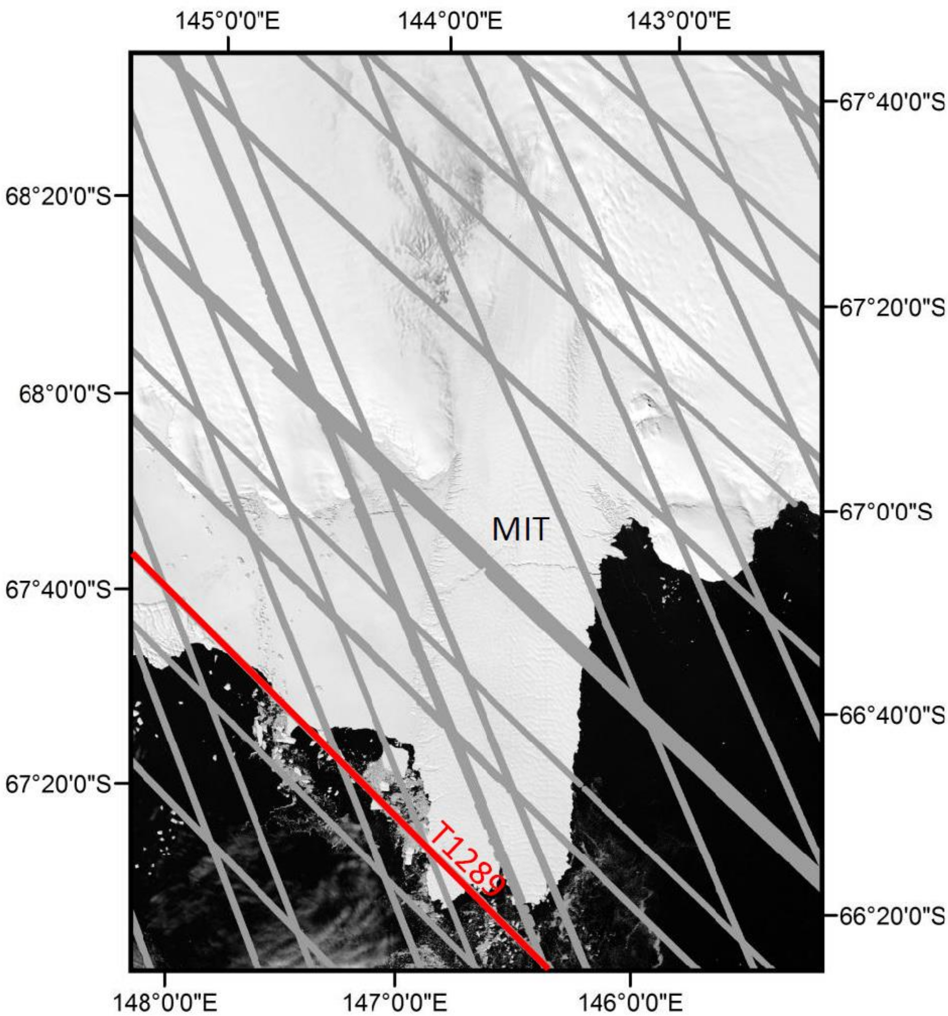

Figure 2. Spatial distribution of ICESat/GLAS data from 2003 to 2009 covering the Mertz region. Ground tracks of ICESat/GLAS are indicated with gray lines. Track 1289 (T1289) is highlighted in red as is used in Figure 6. The background image is from band 4 Landsat 7, captured on February 2, 2003. A polar stereographic projection with -71 °S as standard latitude is used.

The Cryosphere Discuss., doi:10.5194/tc-2016-3, 2016
Manuscript under review for journal The Cryosphere
Published: 21 January 2016

The Cryosphere
Discussions
Open Access

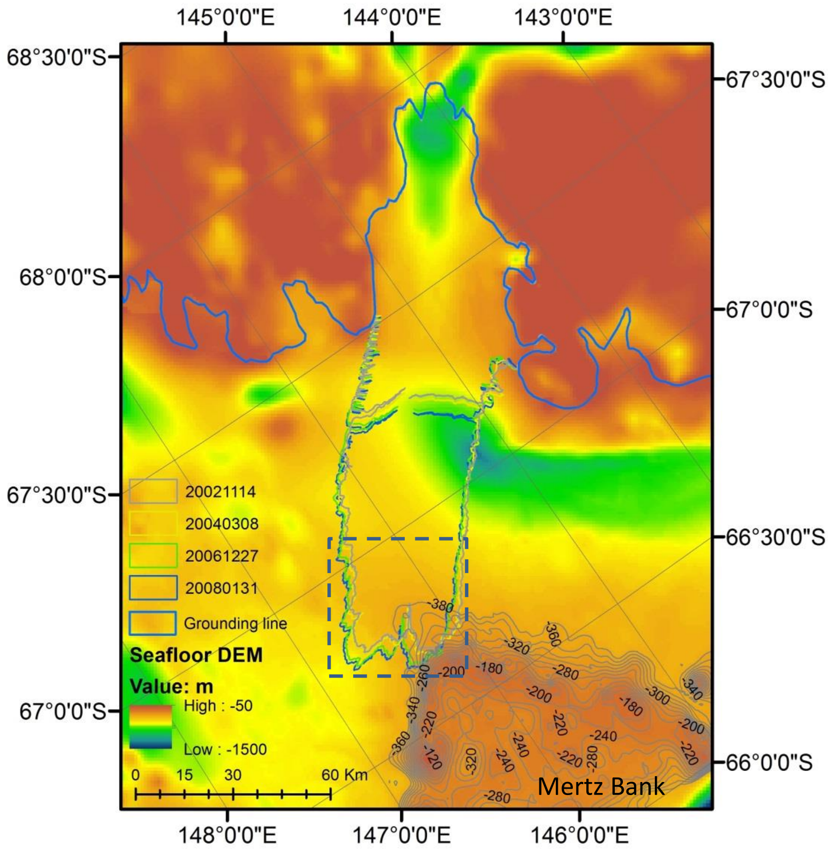

Figure 3. Seafloor topography from bathymetry around Mertz region and outlines of the MIT from 2002 to 2008. The shallow Mertz Bank is located in the lower right (northeast). The blue inset box corresponds to location of Figure 4. The bathymetry measurement profile can be found from S-Figure 1.

The Cryosphere Discuss., doi:10.5194/tc-2016-3, 2016
Manuscript under review for journal The Cryosphere
Published: 21 January 2016

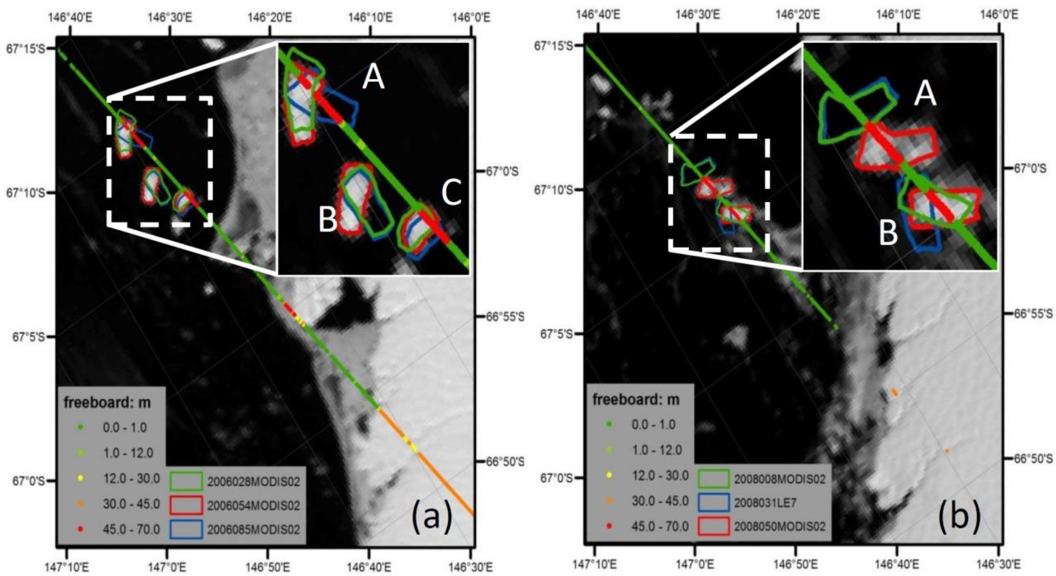

Figure 4. Freeboard extracted from Track 1289, ICESat/GLAS, the location of which can be found in Figure 2 and S-Figure 1. (a) and (b) show the freeboard extracted from ICESat/GLAS on February 23, 2006 (2006054) and February 18, 2008 (2008049) respectively. In each image, positions of three icebergs (with name labeled as 'A', 'B' and 'C') closed to ICESat/GLAS observation time are plotted with green, red and blue polygons respectively. The dates are indicated with seven numbers (yyyyddd) in legend. 'yyyyddd' stands for day 'ddd' in year 'yyyy'. 'MODIS02' and 'LE7' indicate that the image used to extract iceberg outline is from MODIS and Landsat 7 ETM+, respectively.

The Cryosphere Discuss., doi:10.5194/tc-2016-3, 2016
Manuscript under review for journal The Cryosphere
Published: 21 January 2016

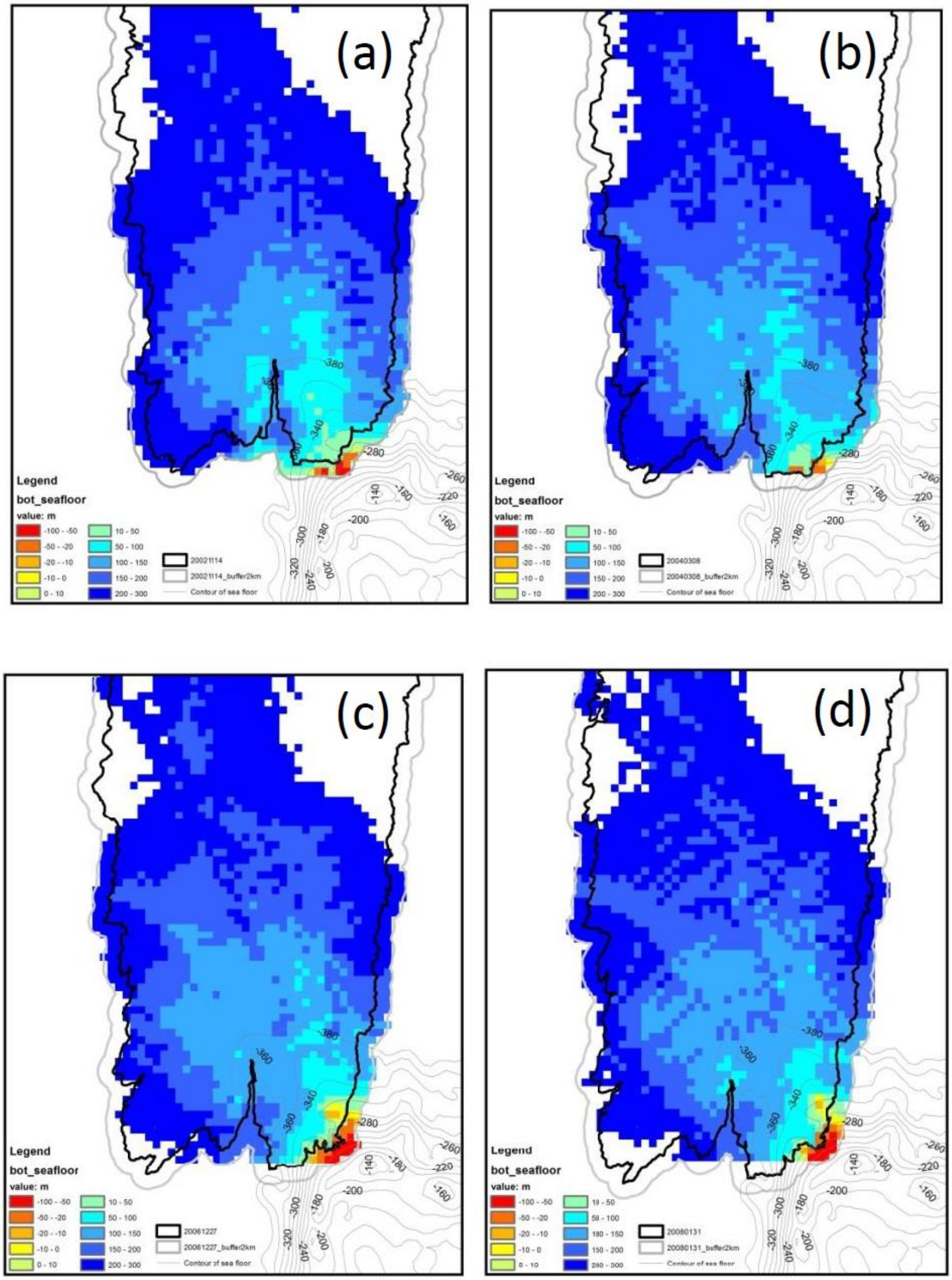

The Cryosphere Discuss., doi:10.5194/tc-2016-3, 2016
Manuscript under review for journal The Cryosphere
Published: 21 January 2016

Figure 5. Elevation difference of Mertz ice bottom and seafloor topography. (a), (b), (c) and (d) correspond to elevation difference assuming hydrostatic equilibrium under the minimum sea surface height -3.35 m on November 14, 2002 , March 8, 2004, December 27, 2006, and January 31, 2008, respectively. The contours in the lower right indicate seafloor topography (unit: m) of the Mertz Bank with an interval of 20 m. The solid black line indicates the boundary of the MIT and the thick gray line outlines a buffer region of the boundary with 2 km as buffer radius. In the legend, negative values mean that ice bottom is lower than the seafloor, which of course is impossible. Therefore, the initial assumption of a floating ice tongue was incorrect in those locations (yellow to red colors), and the ice was grounded. Regions with more negative values indicate more heavily grounding inside of the MIT or more heavily grounding potential in the buffer region.

The Cryosphere Discuss., doi:10.5194/tc-2016-3, 2016
Manuscript under review for journal The Cryosphere
Published: 21 January 2016

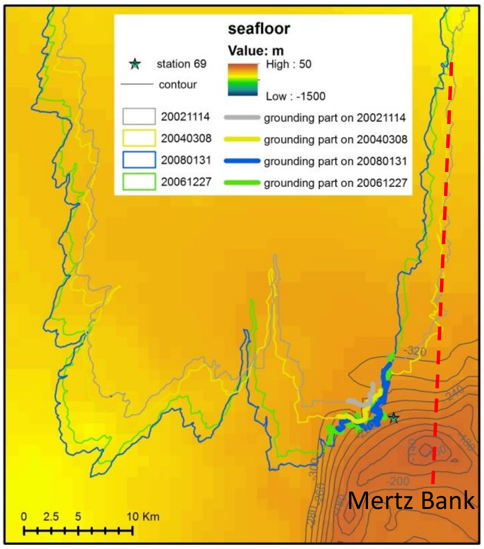

Figure 6. Digital Elevation Map (DEM) of seafloor around Mertz and grounding section of the boundaries extracted from 2002 to 2008. The dashed red line indicates the 'extension line' of the west flank of MIT on November 14, 2002, passing the shallowest region of the Mertz Bank (about -140 m).

The Cryosphere Discuss., doi:10.5194/tc-2016-3, 2016
Manuscript under review for journal The Cryosphere
Published: 21 January 2016

The Cryosphere
Discussions

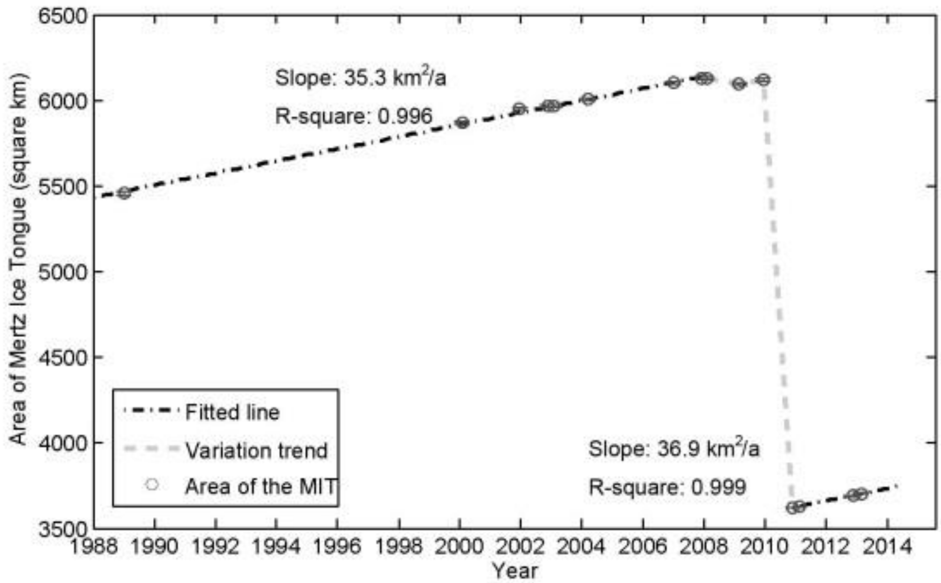

611

612 **Figure 7**. Time series of area change of the MIT. The area covers the entire ice tongue, to the
613 grounding line as indicated with thick blue line in Figure 3. The area is extracted from Landsat
614 images from 1988 to 2013.

Tables

Table 1. Statistics of the three icebergs used to inverse FAC with least-square method. Icebergs 'A', 'B' and 'C' are the same as what are used in Fig. 4.

Icebergs	date	Latitude (°)	Longitude (°)	Freeboard (m)	Seafloor (m)	Sea level (m)	E_{dif} (m)
A	Feb 23, 2006	-67.1737	146.6595	66.88	-528.48	-1.92	7.93
		-67.1752	146.6604	66.34	-527.01	-1.92	10.96
C	Feb 23, 2006	-67.1085	146.6247	66.37	-505.84	-1.92	-10.44
		-67.1100	146.6255	66.28	-507.08	-1.92	-8.44
A	Feb 18, 2008	-67.1194	146.6303	58.88	-522.52	-2.08	69.14
		-67.1209	146.6311	59.58	-524.16	-2.08	64.88
B	Feb 18, 2008	-67.0906	146.6151	67.22	-500.92	-2.08	-22.45
		-67.0921	146.6159	66.10	-500.47	-2.08	-13.55

The Cryosphere Discuss., doi:10.5194/tc-2016-3, 2016
Manuscript under review for journal The Cryosphere
Published: 21 January 2016

The Cryosphere Discussions
Open Access
EGU

Table 2. Statistics of grounding grids inside or grounding potentials outside of the Mertz Ice Tongue (MIT) ('I': inside of thick black line, Fig. 5; 'O': between the black and gray lines, Fig. 5) on November 14, 2002, March 8, 2004, December 27, 2006 and January 31, 2008 respectively. Each grid covers an area of 1 km^2.

Elevation difference (subtracting seafloor from ice bottom)	2002-11-14		2004-03-08		2006-12-27		2008-01-31	
	I	O	I	O	I	O	I	O
17-34(m)	4	5	4	2	7	1	3	5
0-17 (m)	2	6	1	1	6	2	4	2
<0 (m)	0	8	2	5	7	21	6	18
Mean (m)	25.0	-11.9	8.9	-6.4	3.8	-42.1	-0.8	-31.0
Minimum (m)	11.9	-81.5	-46.0	-44.5	-52.3	-102.8	-34.8	-103.0
Standard deviation (m)	8.4	37.8	28.0	27.1	21.8	36.4	19.9	38.0
Number of grids	6	19	7	8	20	22	13	25

The Cryosphere Discuss., doi:10.5194/tc-2016-3, 2016
Manuscript under review for journal The Cryosphere
Published: 21 January 2016

Table 3. Statistics of grounding outlines of the MIT as shown with thick polylines in Fig. 6 on November 14, 2002, March 8, 2004, December 27, 2006 and January 31, 2008 respectively

	2002-11-14	2004-03-08	2006-12-27	2008-01-31
Start location (°)	146.160 °E, 66.689 °S	146.155 °E, 66.681 °S	146.093 °E, 66.700 °S	146.108 °E, 66.695 °S
End location (°)	146.222 °E, 66.689 °S	146.256 °E, 66.683 °S	146.304 °E, 66.669 °S	146.271 °E, 66.675 °S
Perimeter (km)	4.2	6.4	24.7	18.0